JOURNAL OF MATERIALS SCIENCE 31 (1996) 3861–3869

Stress disturbances arising from cut fibre and matrix in unidirectional metal matrix composites calculated by means of a modified shear lag analysis

S. OCHIAI, M. HOJO
Mesoscopic Materials Research Center, Faculty of Engineering, Kyoto University, Sakyo-ku, Kyoto 606, Japan

A useful method to calculate stress disturbances arising from cut fibres is the so-called shear lag analysis, in which it is assumed that fibres act to carry tensile stress without transferring applied stress to the matrix, and the matrix acts to transfer stress to the fibres without carrying tensile stress. This assumption gives a limit for application. In the present work, with unidirectional metal matrix composites in mind, the usual two-dimensional shear lag analysis was modified to express the situation where both fibres and matrix act to carry applied stress and also to transfer stress. By using this modified method, tensile strain concentration in the fibres and matrix adjacent to cut fibres and matrix, and shear stresses at the interface between fibres and matrix, were calculated for some examples.

1. Introduction

The stress disturbances arising from cut fibres in fibre composites has been calculated by the so-called shear lag analysis method, first put forward by Hedgepeth [1]. This method has been proved to give a good description of the stress concentration ahead of the broken fibres when the stiffness of the matrix is low [2] or when the yield stress of the matrix is low [3]. For such cases, this analysis method has been widely employed [4–10].

The shear lag analysis method uses the approximation that fibres act only to carry applied stress without transferring stress to the matrix, and the matrix acts only to transfer stress to the fibres without supporting tensile stress. This approximation, however, limits its application. Only when Young's modulus [2] or yield stress [3] of the matrix is low, can this method be applied successfully. Furthermore, the usual shear lag analysis cannot predict the influence of premature breakage of the matrix, because the tensile stress of the matrix is neglected. On these points, a new approach is needed.

Recently, Ochiai *et al.* [11] presented a new approach applicable to an elastic fibre–elastic matrix composite system, in which both fibres and matrix are treated to act as carriers of tensile stress and also to act as stress-transfer media. The aim of the present work was to develop a calculation method for the stress disturbances in the vicinity of cut fibres and matrix for a two-dimensional elastic fibre–plastically deformable metal matrix composite system, and to show how the strain concentration factor is affected by yield stress of the matrix and also by the breakage of the matrix.

2. Calculation method

2.1. Model composite

A small portion of a two-dimensional composite, in which the cut element(s) (fibre and matrix) and its/their vicinity is/are contained, was taken as schematically shown in Fig. 1. In the present work, three cases shown in Fig. 1 were taken as examples for calculation; (a) one fibre and the surrounding matrices were cut, (b) one fibre was cut but the surrounding matrices were not and (c) one matrix was cut but the surrounding fibres were not. The centre element was numbered 1 and the neighbouring elements 2, 3 to N, outwards. When the number of cut elements was small, the stress disturbances due to cut elements diminish in the elements apart from the cut elements. In this model, the stress in the $N + 1$ elements is approximated to be unaffected by the existence of cut elements. Under this approximation, the strain of the $N + 1$ element is equal to the applied strain on composites, e.

The displacements at the centre line of 1 to $N + 1$ elements were denoted as U_1 to U_{N+1}, respectively, the displacements of the interface between i and $i + 1$ elements as $U_{i/i+1}$, the shear stress at the interface between i and $i + 1$ as $\tau_{i/i+1}$, as shown in Fig. 2. The distance, x, was taken from the cut-ends of elements in the longitudinal direction, as shown in Fig. 1. Under this notation, U_{N+1} was expressed as *ex.* U_i, $U_{i/i+1}$ and $\tau_{i/i+1}$ ($i = 1$–N) vary with x. The width, Young's modulus and shear modulus of fibres were denoted d_f, E_f and G_f, respectively, those of matrix as d_m, E_m and G_m, respectively, and the thickness of the present composite as h.

0022–2461

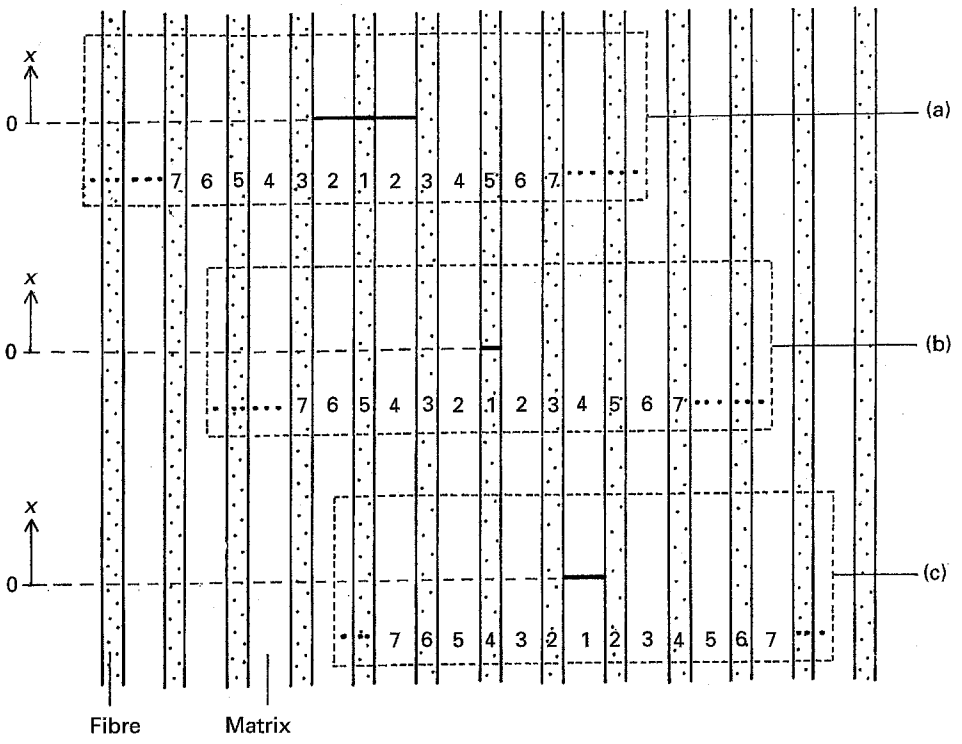

Figure 1 Schematic representation of cases (a)–(c).

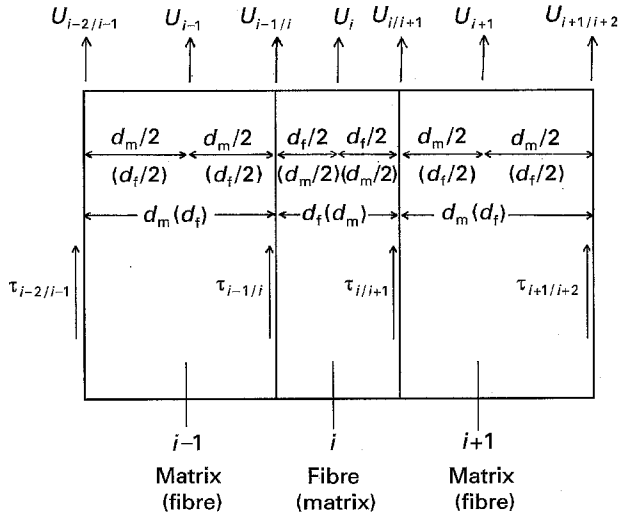

Figure 2 Notation of U_i, $U_{i/i+1}$ and $\tau_{i/i+1}$. The subscripts i and $i/i+1$ refer to the ith element and $i/i+1$ interface, respectively.

2.2. Simplification of the stress–strain curve of the matrix

The tensile stress–strain, σ_m–e, curve of the matrix was expressed as follows based on the approximation that the matrix shows linear strain hardening after yielding

$$\sigma_m = eE_m \quad \text{for } e < e_y \tag{1}$$

$$\sigma_m = (1-\alpha)\sigma_y + \alpha e E_m \quad \text{for } e >= e_y \tag{2}$$

where E_m is the Young's modulus, e_y the yield strain, σ_y the yield stress given by $e_y E_m$ and α the slope of the stress–strain curve in the stage of plastic deformation, normalized with respect to E_m. Similarly, the shear stress – shear strain, τ–γ curve was approximated as

$$\tau_m = G_m\gamma \quad \text{for } \gamma < \gamma_y \tag{3}$$

$$\tau m = (1-\beta)\tau_y + \beta G_m\gamma \quad \text{for } \gamma > \gamma_y \tag{4}$$

where γ_y is the shear yield strain, τ_y the shear yield stress given by $G_m\gamma_y$ and β the slope of the shear stress – shear strain curve, normalized with respect to G_m. β is approximately given by [12]

$$\beta = \alpha E_m/(4G_m) \tag{5}$$

2.3. Shear stresses acting at the interface

When the absolute value of interfacial shear stress at the $i/i+1$ interface, $|\tau_{i/i+1}|$, shown in Fig. 2, is lower than τ_y, the $i/i+1$ interface is termed the elastic interface. In this case, $\tau_{i/i+1}$ can be expressed as

$$\tau_{i/i+1} = G_f(U_{i+1} - U_{i/i+1})/(d_f/2) = G_m(U_{i/i+1} - U_i)/(d_m/2) \tag{6}$$

by applying Dow's approximation [13] for the case where element i corresponds to fibres. From Equation 6, we have

$$\tau_{i/i+1} = H(U_{i+1} - U_i) \tag{7}$$

$$H = 2G_fG_m/(d_fG_m + G_fd_m) \tag{8}$$

For the case where i corresponds to the matrix, $\tau_{i/i+1}$ can be calculated in a similar manner, also being expressed by Equations 7 and 8.

When $|\tau_{i+i+1}|$ is higher than τ_y, the $i/i+1$ interface is termed the plastic interface. In this case, $\tau_{i/i+1}$ can be expressed by using Equation 4 as

$$\tau_{i/i+1} = G_f(U_{i+i} - U_{i/i+1})/(d_f/2) = (1-\beta)\tau_y + \beta G_m(U_{i/i+1} - U_i)/(d_m/2) \tag{9}$$

From Equation 9, we have

$$\tau_{i/i+1} = J(U_{i+1} - U_i) + \tau_{y'} \tag{10}$$

$$J = 2\beta G_fG_m/(\beta d_fG_m + G_fd_m) \tag{11}$$

$$\tau_{y'} = G_fd_m(1-\beta)\tau_y/(\beta d_fG_m + G_fd_m) \tag{12}$$

Equations 7 and 10 for elastic and plastic interfaces, respectively, can be expressed in the general form given by

$$\tau_{i/i+1} = J_{i/i+1}(U_{i+1} - U_i) + \tau_{y'i/i+1} \quad (13)$$

where the $J_{i/i+1}$ and $\tau_{y',i/i+1}$ are given by H and zero, respectively, for an elastic interface, and they are given by J and $\tau_{y'}$, respectively, for a plastic interface.

2.4. Stress equilibrium equations

The stiffness ratio of the matrix to fibre, μ, expressed by Equation 14, was introduced in this work for convenience

$$\mu = E_m d_m/(E_f d_f) = E_m V_m/(E_f V_f) \quad (14)$$

where V_f and V_m are volume fractions of fibre and matrix, respectively, given by

$$V_f = d_f/(d_f + d_m) \quad (15a)$$

$$V_m = d_m/(d_f + d_m) \quad (15b)$$

The stress equilibrium can be expressed as

$$\alpha_i \mu_i d_f h E_f (d^2U_i/dx^2) + h(\tau_{i/i+1} - \tau_{i-1/i}) = 0 \quad (16)$$

For a fibre, α_i and μ_i are unity for any value of i. For the matrix, α_i is given by α and 1 for plastic and elastic matrices, respectively, and μ_i is given by μ.

Combining Equations 13 and 16, we have the general expression for stress equilibrium

$$\begin{aligned}\alpha_i \mu_i d_f h E_f (d^2U_i/dx^2) + [&J_{i/i+1}U_{i+1} \\ &- (J_{i/i+1} + J_{i-1/i})U_i \\ &+ J_{i-1/i}U_{i-1} + \tau_{y',i/i+1} - \tau_{y',i-1/i}] = 0\end{aligned} \quad (17)$$

In the present calculation, as the number of breakages of fibres and matrix is small, the fibres and matrix away from the broken elements were assumed to be unaffected, as stated above. The number of affected elements is denoted N. (N was taken to be 7 in the present calculation. If N was taken to be more, the calculation results were essentially the same.) As $i = 1$ is taken to be the centre of the region picked up in this work as shown in Fig. 1, Equation 17 can be rewritten as

$$d^2U_1/dx^2 + \xi_1[2J_{1/2}(U_2 - U_1) + 2\tau_{y',1/2}] = 0 \quad (18a)$$

$$\begin{aligned}d^2U_i/dx^2 + \xi_i[&J_{i/i+1}U_{i+1} - (J_{i/i+1} + J_{i-1/i}) \\ &\times U_i + J_{i-1/i}U_{i-1} \\ &+ \tau_{y',i/i+1} - \tau_{y',i-1/i}] = 0 \quad (i = 2\text{–}N)\end{aligned} \quad (18b)$$

$$\begin{aligned}d^2U_N/dx^2 + \xi_N[&J_{N/N+1}ex - (J_{N/N+1} + J_{N-1/N})U_N \\ &+ J_{N-1/N}U_{N-1} + \tau_{y',N/N+1} - \tau_{y',N-1/N}] = 0\end{aligned} \quad (18c)$$

where $\xi_i = 1/\alpha_i \mu_i d_f E_f$ for $i = 1$–N.

2.5. Stages arising during deformation

The parameters of α_i, $J_{i/i+1}$ and $\tau_{y'i/i+1}$ vary depending on the situation of matrix and interface. If the matrix i behaves elastically in tension, α_i is given by 1, and when it behaves plastically, α_i is given by α. When interface $i/i+1$ is elastic, $J_{i/i+1}$ and $\tau_{y'i/i+1}$ are given by H and 0, respectively, and when it is plastic, they are given by J and $\tau_{y'}$, respectively. In this way, Equations 18 can be applied to various cases by substituting appropriate values into α_i, μ_i, $J_{i/i+1}$ and $\tau_{y'i/i+1}$.

As the matrix is a plastically deformable metal in the present work, the calculation will be performed only for the deformation stage, where the matrix at infinity ($x = \infty$) has already yielded. The calculation results for the deformation stage where the matrix deforms elastically have been reported in our former work [11].

In the three examples shown in Fig. 1a–c, the situations of matrix and interface vary as shown in Figs 3, and 4a and b, and 4c and d, respectively.

Case (a) (Fig. 3): one fibre (1) and neighbouring matrices (2) are cut. The matrices other than 2 are plastic in tension in the whole range of x, and the matrix 2 is elastic for $0 \leqslant x \leqslant b$ but plastic for $b \leqslant x$, where b is the dimension of the elastic matrix, which is infinite when the applied strain on the composite as a whole is equal to the yield strain of the matrix, but decreases with increasing applied strain, e. On the other hand, the dimension of the plastic interface 2/3, a, increases with increasing applied strain. Therefore, b is larger than a at low applied strain, as schematically shown in Fig. 3a (Stage I), but the former becomes smaller than the latter at higher applied strain as shown in Fig. 3b (Stage II). All interfaces other than 2/3 are elastic and the interface 2/3 is plastic for $0 \leqslant x \leqslant a$ but elastic for $a \leqslant x$. With further increasing applied strain e, the 1/2 interface becomes plastic as shown in Fig. 3c (Stage III). In this stage, the interfaces 1/2 and 2/3 are plastic for $0 \leqslant x \leqslant c$ where c is the dimension of the plastic interface of 1/2, only 2/3 is plastic for $c \leqslant x \leqslant a$. In this way, there arise many stages, depending on applied strain.

In each stage, many regions arise as schematically shown in Fig. 3. For instance, in Stage I, Regions A–C arise as shown in Fig. 3. In Region A, all matrix elements (2, 4, 6, ...) are plastic and all interfaces are elastic. Therefore, $\alpha_i = \alpha$ for matrix elements (2, 4, 6, ...) and 1 for fibre elements (1, 3, 5 ...), and $J_{i/i+1} = H$ and $\tau_{y'i/i+1} = 0$ for $i = 1$–N. In Region B, α_2 becomes unity, but other parameters of $\alpha_i (i \neq 2)$, $J_{i/i+1}(i = 1\text{–}N)$ and $\tau_{y'i/i+1}(i = 1\text{–}N)$ are the same as those in Region A. In Region C, $J_{2/3}$ becomes J, and $\tau_{y'2/3}$ becomes $\tau_{y'}$ but other parameters are the same as those in Region B. Also for Stages II and III, the parameters for each region can be given in a similar manner.

Case (b) (Fig. 4a and b): one fibre denoted 1 is cut. All matrices have yielded in tension. At low applied strain, all interfaces except 1/2 are elastic in shear. The interface 1/2 is plastic for $0 \leqslant x \leqslant f$ but elastic for $f \leqslant x$, as shown in Fig. 4a. f increases with increasing

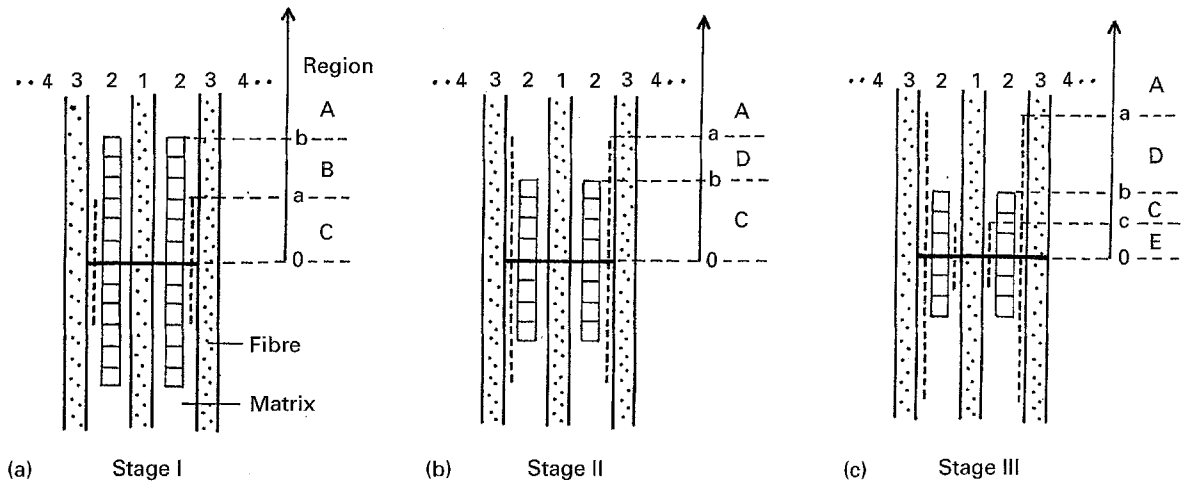

Figure 3 Schematic representation of deformation stages I–III and Regions A–E which appear during deformation for case (a). In this case, 1, 3, 5, ..., correspond to fibre and 2, 4, 6, ..., to matrix. The broken lines at the 1/2 and 2/3 interfaces correspond to plastic interfaces and other interfaces without broken lines correspond to elastic interfaces. The matrix 2 for $0 \leqslant x \leqslant b$ deforms elastically in tension. The matrix 2 for $b \leqslant x$ and matrices 4, 6, ..., at any x deform plastically in tension.

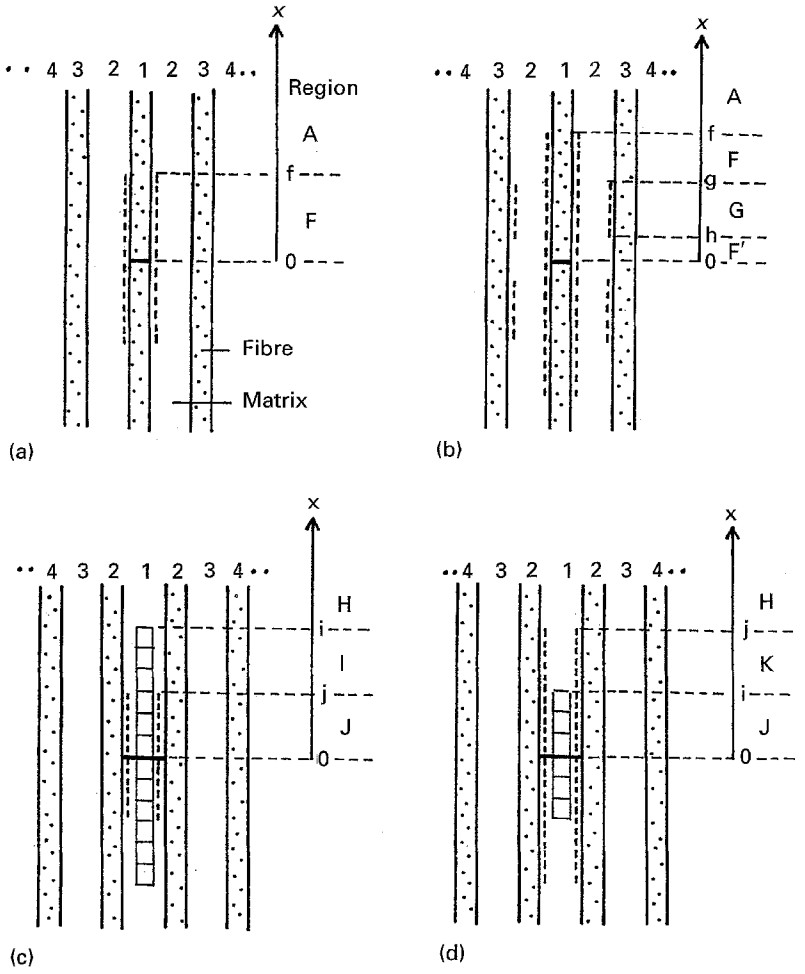

Figure 4 Schematic representation of deformation stages and regions which appear during deformation (a, b) for case (b) and (c, d) for case (c).

applied strain. With further increasing applied strain, the interface 1/2 becomes plastic for $h \leqslant x \leqslant g$ as shown in Fig. 4b.

Case (c) (Fig. 4c and d): one matrix denoted 1 is cut. All matrices other than 1 are plastic in tension and the matrix 1 is elastic for $0 \leqslant x \leqslant i$ but plastic for $i \leqslant x$. All interfaces other than 1/2 are elastic and the interface 1/2 is plastic for $0 \leqslant x \leqslant j$ but elastic for $j \leqslant x$. In this case, as well as in case (a), i is larger than j at low applied strain, as shown in Fig. 4c but becomes smaller as in Fig. 4d.

In this work, we denote the regions which appear during deformation as A,B,... and J, as shown in Figs 3 and 4. The values of α_i, μ_i, $J_{i/i+1}$ and $\tau_{y'i/i+1}$ for each region can be given as typically shown in Table I for case (a).

TABLE I Values of α_i, μ_i, $J_{i/i+1}$ and $\tau_{y'i/i+1}$ for Regions A–E in case (a) shown in Fig. 3

Region	α_i	μ_i	$J_{i/i+1}$	$\tau_{y'i/i+1}$
A	$\alpha_i = 1$ for i = odd $\alpha_i = \alpha$ for i = even	$\mu_i = 1$ for i = odd $\mu_i = \mu$ for i = even	$J_{i/i+1} = H$ for $i = 1$–N	$\tau_{y'i/i+1} = 0$ for $i = 1$–N
B	$\alpha_i = 1$ for i = odd $\alpha_2 = 1$ $\alpha_i = \alpha$ for i = even except 2	$\mu_i = 1$ for i = odd $\mu_i = \mu$ for i = even	$J_{i/i+1} = H$ for $i = 1$–N	$\tau_{y'i/i+1} = 0$ for $i = 1$–N
C	$\alpha_i = 1$ for i = odd $\alpha_2 = 1$ $\alpha_i = \alpha$ for i = even except 2	$\mu_i = 1$ for i = odd $\mu_i = \mu$ for i = even	$J_{2/3} = J$ $J_{i/i+1} = H$ for $i = 1$–N except 2	$\tau_{y'2/3} = \tau_{y'}$ $\tau_{y'i/i+1} = 0$ for $i = 1$–N except 2
D	$\alpha_i = 1$ for i = odd $\alpha_i = \alpha$ for i = even	$\mu_i = 1$ for i = odd $\mu_i = \mu$ for i = even	$J_{2/3} = J$ $J_{i/i+1} = H$ for $i = 1$–N except 2	$\tau_{y'2/3} = \tau_{y'}$ $\tau_{y'i/i+1} = 0$ for $i = 1$–N except 2
E	$\alpha_i = 1$ for i = odd $\alpha_2 = 1$ $\alpha_i = \alpha$ for i = even except 2	$\mu_i = 1$ for i = odd $\mu_i = \mu$ for i = even	$J_{i/i+1} = J$ for $i = 1$ and 2 $J_{i/i+1} = H$ for $i = 3$–N	$\tau_{y'i/i+1} = \tau_{y'}$ for $i = 1$ and 2 $\tau_{y'i/i+1} = 0$ for $i = 3$–N

2.6. General solutions

General solutions for Equations 18 for Regions A–K are expressed as follows

$$U_i^{(R)} = ex + \sum_{k=1}^{N} \{\tau_{y',k/k+1}/J_{k/k+1}\} + \sum_{j=1}^{2N} A_j^{(R)} B_{i,j}^{(R)} \exp(c_j^{(R)} x) \quad (19)$$

where the superscripts (R) refer to Regions A–K. $A_j^{(R)}$s are unknown constants which should be solved from boundary conditions. $c_j^{(R)}$ for $j = 1$–$2N$ are constants, among which the relation of $c_{j+N}^{(R)} = -c_j^{(R)}$ is held for $j = 1$–N. $\{c_j^{(R)}\}^2$s are eigen values of the matrix $T_N^{(R)}$ given by

$$T_N^{(R)} = \begin{bmatrix} 2\xi_1 j_{1/2} & -2\xi_1 J_{1/2} & & & \\ -\xi_2 J_{1/2} & \xi_2(J_{1/2}+J_{2/3}) - \xi_2 J_{2/3} & & & \\ & \cdots\cdots\cdots\cdots\cdots\cdots & & & \\ & -\xi_i J_{i-1/i} & \xi_i(J_{i-1/i}+J_{i/i+1}) & -\xi_i J_{i/i+1} & \\ & \cdots\cdots & & & \\ & & -\xi_N J_{N-1/N} & \xi_N(J_{N-1/N}+J_{N/N+1}) & \end{bmatrix} \quad (20)$$

and $B_{i,j}^{(R)}$'s are constants given by

$$B_{1,j}^{(R)} = 1 \qquad (j = 1\text{–}2N) \quad (21a)$$

$$B_{2,J}^{(R)} = B_{1,j}^{(R)}\{1 - (c_j^{(R)})^2/(2J_{1/2}\xi_1)\} \qquad (j = 1\text{–}2N) \quad (21b)$$

$$B_{i,j}^{(R)} = B_{i-1,j}^{(R)}\{-(c_j^{(R)})^2/\xi_{i-1} + (J_{i-2/i-1} + J_{i-1/i})/J_{i-1/i}\}/J_{i-1/i} - B_{i-2,j}^{(R)}(J_{i-2/i-1}/J_{i-1/i}) \quad (j = 1\text{–}2N, i = 3\text{–}N) \quad (21c)$$

2.7. Boundary conditions

The unknown values $A_j^{(R)}$s and a, b, c, f, g, h, i and j shown in Figs 3 and 4 can be solved numerically by giving the following boundary conditions.

(A) At $x = 0$, the strains of cut fibre and matrix are zero, and the displacements of uncut fibres and matrix are zero.

(B) At $x = a, b, \ldots, j$, the displacements and the strains of all elements are continuous.

(C) At $x = a, c, f, g, h$ and j, the shear stresses at 2/3 (Stages I–III in Fig. 3), 1/2 (Stage III in Fig. 3), 1/2 (Fig. 4a and b), 2/3 (Fig. 4b), and 1/2 (Fig. 4c and d) interfaces, are equal to the shear yield stress of the matrix.

(D) At $x = b$ in Fig. 3 and at $x = i$ in Fig. 4c and d, tensile stresses of the matrix 2 and 1, respectively, are equal to the tensile yield stress of the matrix.

(E) At $x = \infty$, the strain is equal to e in each element.

The number of unknown values is dependent on deformation stage. Taking Stage I in case (a) shown in Fig. 3a as an example, the unknown values are $A_1^{(A)}$ to $A_{2N}^{(A)}$, $A_1^{(B)}$ to $A_{2N}^{(B)}$, $A_1^{(C)}$ to $A_{2N}^{(C)}$, a and b. The total unknown values are $6N + 2$. The boundary conditions A–E are expressed by the following equations

$$(A)\, U_i^{(C)} = 0 \qquad \text{for } i = 3\text{–}N \quad (22a)$$

and

$$dU_i^{(C)}/dx = 0 \qquad \text{for } i = 1 \text{ and } 2 \quad (22b)$$

$$(B)\ U_i^{(A)}(b) = U_i^{(B)}(b),\ dU_i^{(A)}(b)/dx = dU_i^{(B)}(b)/dx,\ U_i^{(B)}(a) = U_i^{(C)}(a) \quad (23a)$$

and

$$dU_i^{(B)}(a)/dx = dU_i^{(C)}(a)/dx \qquad \text{for } i = 1\text{–}N \quad (23b)$$

$$(C)\ H\{U_2^{(B)}(a) - U_1^{(B)}(a)\} = -\tau_y \quad (24)$$

(as shear stress acts in the $-x$ direction, we express shear stress to be positive for the $-x$ direction)

$$(D)\ E_m\{dU_2^{(A)}(b)/dx\} = \sigma_y \quad (25)$$

$$(E)\ dU_i^{(A)}(\infty)/dx = e \qquad \text{for } i = 1\text{–}N \quad (26)$$

Thus $6N + 2$ equations can be obtained. From these equations, $6N + 2$ unknown values can be calculated

TABLE II Values of mechanical properties of fibre and matrix used in the present calculation. The width and volume fraction of fibre were taken to be 0.1 mm and 0.5, respectively

Mechanical properties	Fibre	Matrix		
		S1	S2	S3
Young's modulus (GPa)	400	100	200	200
Shear modulus (GPa)	160	30	60	60
Tensile strain-hardening coefficient normalized with respect to Young's modulus, α	–	0.02	0.02	0.02
Tensile yield stress (MPa)	–	200	400	800
Shear yield stress (MPa)	–	100	200	400

numerically. The strain concentration, $K_i(x)$, at $x = x$ for element i is expressed as

$$K_i(x) = \{dU_i^{(R)}(x)/dx\}/e \quad (27)$$

It was difficult to calculate exact values of more than three of $a, b, \ldots$ and j because they are contained in the exponential terms. For this reason, calculation for stage III for case (a) in Fig. 3 and (b) in Fig. 4 was not performed in the present work.

The calculation was done by using the values listed in Table II. The width of fibre, d_f, was taken to be 0.1 mm and the volume fraction of fibre to be 0.5. In order to determine the influence of Young's modulus and yield stress of the matrix on the stress disturbances, three types of matrix, S1–S3, were taken as examples. The S1–S3 matrices refer to relatively soft, medium and hard metals, respectively, as shown in Table II.

3. Results and discussion

3.1. Case (a)

Typical tensile and shear-stress distributions as a function of x for case (a) are shown in Figs 5 and 6, respectively, in which the results for the S1–S3 matrices are shown in (a)–(c), respectively. In this example, the applied strain was 0.5%, which corresponded to Stages II, II and I for S1–S3 matrices, respectively. Regions A, D and C in Stage II for S1 matrix covered $0.78(=a) \leqslant x$, $0.59(=b) \leqslant x \leqslant 0.78$, and $0 \leqslant x \leqslant 0.59$, respectively, and those for S2 matrix covered $0.49(=a) \leqslant x$, $0.46(=b) \leqslant x \leqslant 0.49$ and $0 \leqslant x \leqslant 0.46$, respectively (in mm). Regions A, B and C in Stage I for S3 matrix corresponded to $0.55(=b) \leqslant x$, $0.24(=a) \leqslant x \leqslant 0.55$ and $0 \leqslant x \leqslant 0.24$, respectively (mm). Figs 5 and 6 give the following indications.

(1) The strain concentration factor for all elements is highest at $x = 0$ but it decreases with increasing x and then increases, approaching 1 (unity) at large x.

(2) The smaller the i, that is the shorter the distance from the cut elements in the transverse direction, the higher becomes the strain concentration around $x = 0$. The decrease in strain concentration factor with increasing x is also large when i is small in the range of $x \leqslant 0.5$ mm.

(3) The harder the matrix, the higher becomes the strain concentration factor at $x = 0$, which cannot be predicted by the unusual shear lag analysis.

(4) The shear stress at the 2/3 interface is highest at $x = 0$ and it decreases gradually for $x \leqslant a$ (corresponding to the plastic interface region) and then rapidly for $x \geqslant a$ (corresponding to the elastic interface region).

(5) The shear stress at the 1/2 interface decreases and then increases, but then again decreases with increasing x for the S1 matrix while it only decreases for the S3 matrix. However, this feature is not fixed but is dependent on applied strain. Further calculation revealed that the shear stress for the S3 matrix shows the same tendency as that for the S1 matrix when the applied strain becomes high.

(6) According to the usual shear lag analysis, $\tau_{1/2}$ and $\tau_{2/3}$ are treated as being the same. However, the present results indicate that the difference between these two shear stresses is large when the matrix is hard (S3). On the other hand, when the matrix is soft (S1), the difference becomes relatively small, according to which the usual shear lag analysis will yield similar results to the present method.

(7) The differences between $\tau_{3/4}$ and $\tau_{4/5}$ and that between $\tau_{5/6}$ and $\tau_{6/7}$ were very small, and cannot be distinguished on the scale in Fig. 6.

(8) $\tau_{3/4}$ to $\tau_{6/7}$ were zero at $x = 0$ but they increased, reaching a maximum and then decreased with increasing x.

As it was found that the strain concentrations for uncut elements $(3, 4, 5, \ldots)$ are highest at $x = 0$, the variation of strain concentration at $x = 0$, $K_i(0)$, was calculated as a function of applied strain, e. A typical result for the S3 matrix is presented in Fig. 7. There are three distinct features.

(i) In case of elastic matrix composites, the strain concentration factor is independent of applied strain [1, 2, 10, 11]. On the other hand, in the plastically deformable metal matrix composites, it varies with increasing applied strain.

(ii) The strain concentration in the elements near the cut elements, such as $K_3(0)$ and $K_4(0)$, decrease with increasing e. Therefore, the probability of breakage of fibres (3) in metal matrix composites becomes low in comparison with that in elastic matrix composites. This is one of the advantages of metal matrix composites.

(iii) The changes in $K_i(0)$ for the elements apart from cut elements such as $K_6(0)$ and $K_7(0)$ with increasing applied strain are small in comparison with those of $K_3(0)$ and $K_4(0)$. As a result, the difference

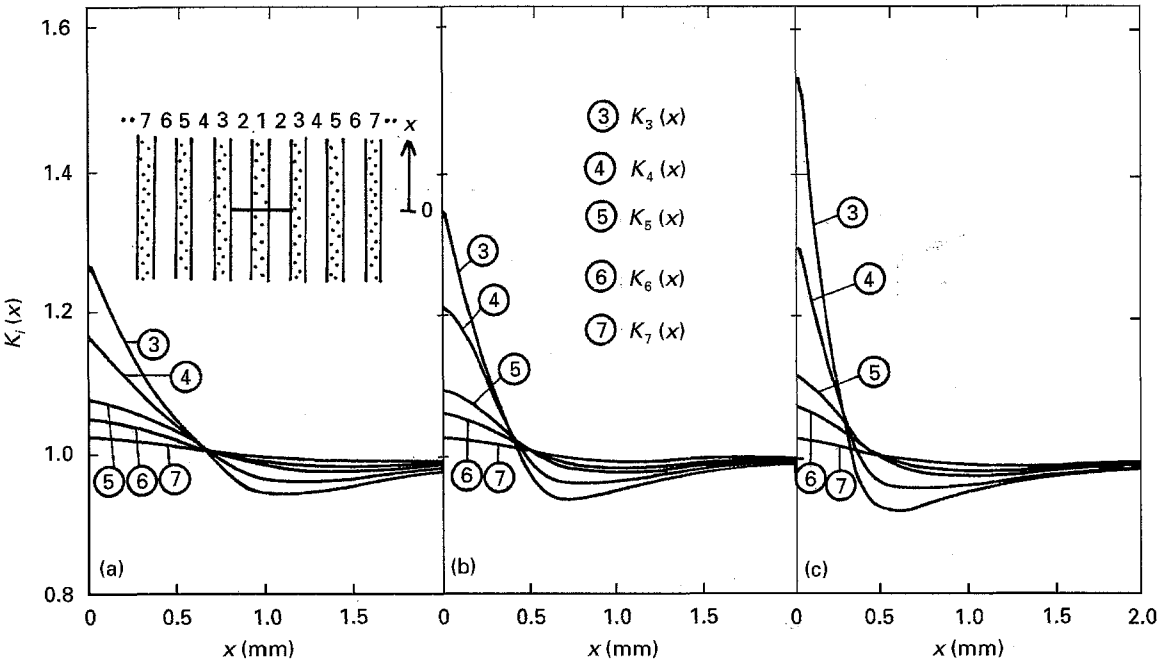

Figure 5 Variations of strain concentration factor $K_i(x)$ ($i = 3$–7) as a function of x at $e = 0.5\%$ in case (a) for (a) S1, (b) S2 and (c) S3 matrices.

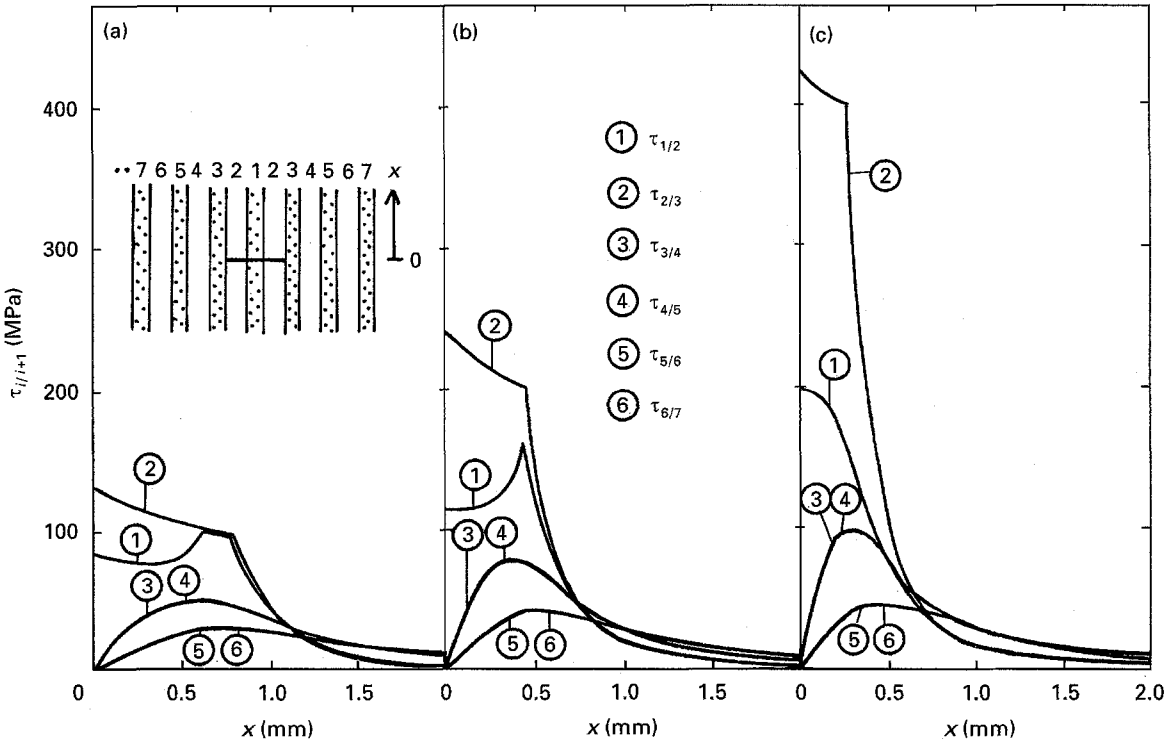

Figure 6 Variations of shear stress $\tau_{i/i+1}(x)$ ($i = 1$–6) as a function of x at $e = 0.5\%$ in case (a) for (a) S1, (b) S2 and (c) S3 matrices.

in $K_i(0)$ among the elements becomes small at high applied strain.

Fig. 8 shows a comparison of the results of the present shear lag analysis with those of the usual one. The difference is relatively small for the soft S1 matrix as shown in Fig. 8, but it becomes large for harder S2 and S3 matrices Fig. 8(b, c). This result indicates that the usual shear lag analysis is useful to calculate strain concentration factors for soft metal matrix composites, but not for hard and stiff matrix composites.

3.2. Case (b)

The difference in the strain concentration factor between cases (a) and (b) was relatively small when the matrix was soft. However, the difference became large when the matrix was hard and stiff. Figs 9 and 10 show a comparison of $K_i(x)$ and $\tau_{i/i+1}$ between cases (a) and (b), respectively, for the S3 matrix. Figs 9 and 10 give the following indications.

(1) The strain concentration factors $K_i(x)$ for all elements around $x = 0$ in case (a) are higher than those in case (b). This means that the existence of

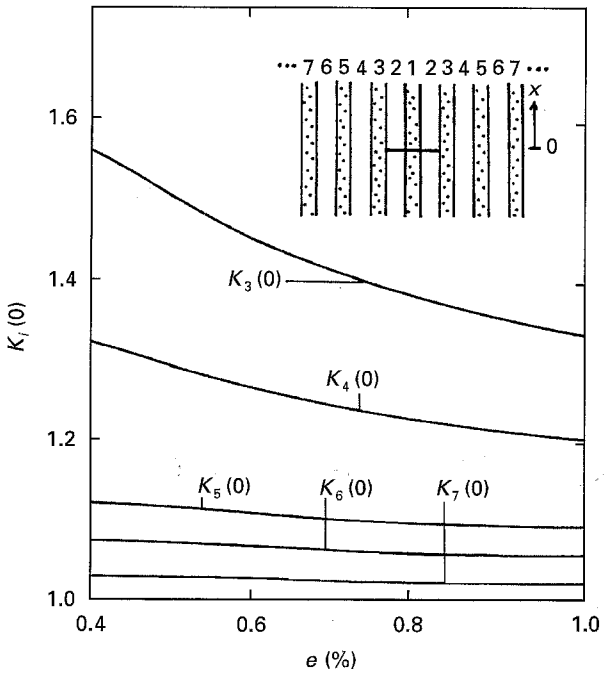

Figure 7 Variations of strain concentration factor $K_i(0)$ $(i = 3–7)$ as a function of applied strain e in case (a) for S3 matrix.

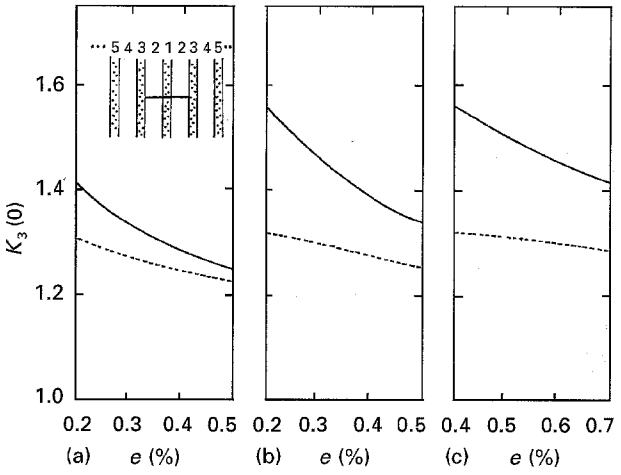

Figure 8 Variations of $K_3(0)$ as a function of applied strain e for (a) S1, (b) S2 and (c) S3 matrices (———) calculated by the present shear lag analysis, together with (···) those calculated by the usual shear lag analysis for comparison.

uncut matrices surrounding the cut fibre acts to reduce the strain concentration factor.

(2) In case (b), the shear stress $\tau_{i/i+1}$ around $x = 0$ is highest at the 1/2 interface, while in case (a), the shear stress was highest at the 2/3 interface.

(3) The variation of $\tau_{2/3}$ is quite different between cases (a) and (b). In case (b), $\tau_{2/3}$ is zero at $x = 0$ and then increases very rapidly, reaching a maximum, and decreases with increasing x, while in case (a), it is highest at $x = 0$ and decreases with increasing x.

(4) The differences between $\tau_{3/4}$ and $\tau_{4/5}$ and between $\tau_{5/6}$ and $\tau_{6/7}$ are very small over the whole range of x for both cases (a) and (b). The difference between $\tau_{1/2}$ and $\tau_{2/3}$ is large at small x but it becomes very small at large x for both cases (a) and (b).

Fig. 11 shows the variation of $K_i(0)$ as a function of e for the S3 matrix in case (b). It is important that the strain concentration on matrix 2 is very high in comparison with that on other elements. This indicates that the matrix 2 could be broken if the failure strain of matrix is low. Once the matrix 2 is broken, the stress concentration on fibre 3 becomes high, as shown in the results for case (a).

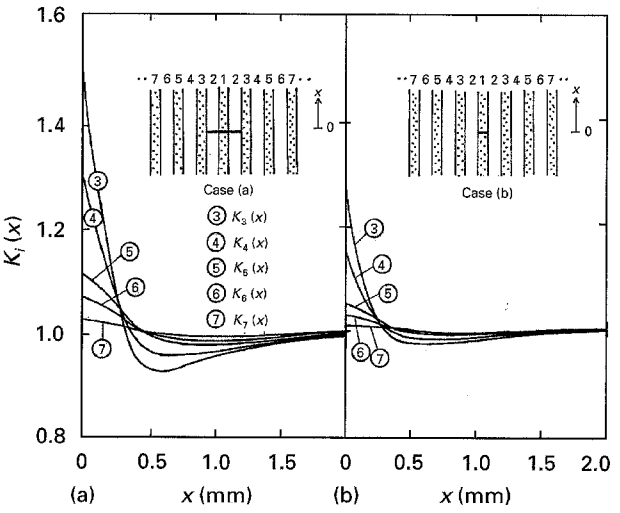

Figure 9 Comparison of variations of $K_i(x)$ $(i = 3–7)$ for S3 matrix at $e = 0.5\%$ between cases (a) and (b).

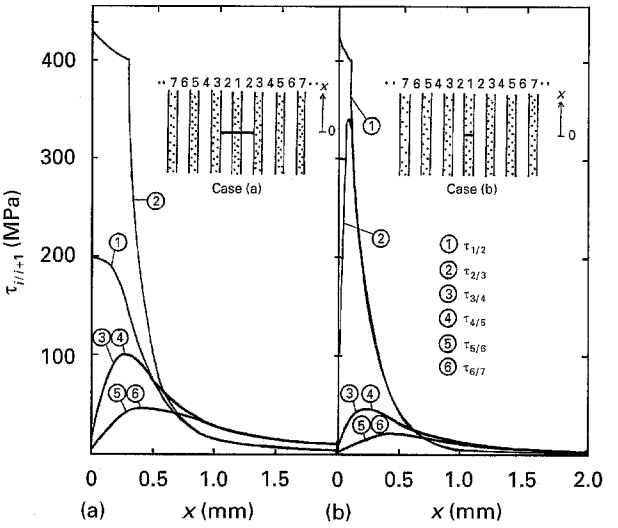

Figure 10 Comparison of variations of $\tau_{i/i+1}(x)$ $(i = 1–6)$ for S3 matrix at $e = 0.5\%$ between cases (a) and (b).

Fig. 12 shows a comparison of $K_3(0)$ for the S3 matrix in case (b) with that for case (a), together with the results based on the usual shear lag analysis. The existence of uncut matrix 2 in case (b) reduces the strain concentration factor on fibre 3. The strain concentration factor is lower than that calculated by the usual shear lag analysis and is very much lower than that for case (a). As the matrix is hard in this example (S3 matrix), $K_3(0)$ is strongly dependent on it, whether or not the matrix 2 is cut. In order to achieve high-strength composites, the matrix should have a high failure strain. This indication cannot be obtained by the usual shear lag analysis.

3.3. Case (c)

Fig. 13 shows the influence of the cut matrix on the strain concentration factor of the neighbouring fibres

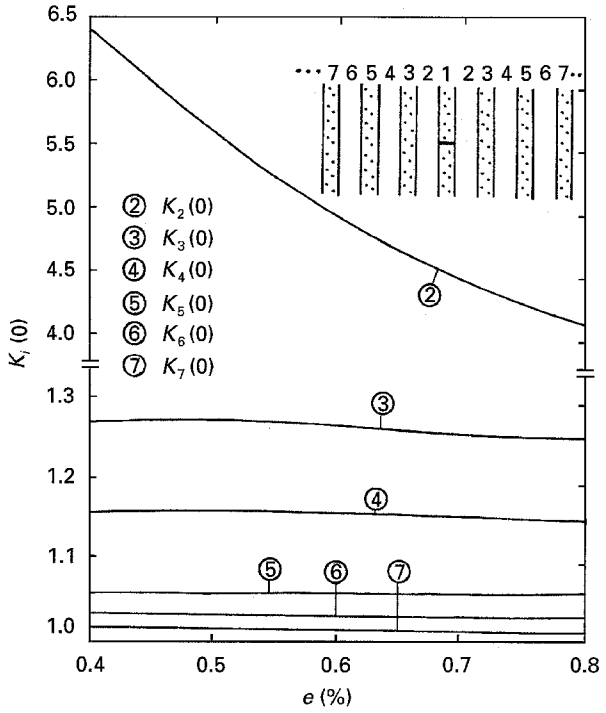

Figure 11 Variations of $K_i(0)$ ($i = 2$–7) as a function of applied strain e in case (b) for the S3 matrix.

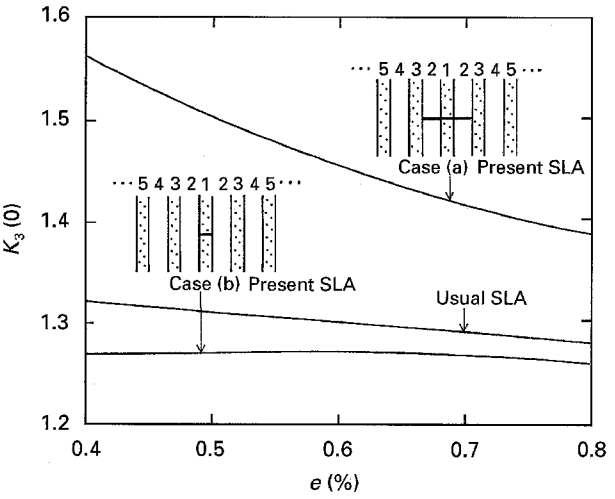

Figure 12 Comparison of $K_3(0)$ for S3 matrix calculated by the present shear lag analysis for cases (a) and (b) with that calculated by the usual shear lag analysis.

2. The strain concentration factor decreases with increasing applied strain. It should be noted that the harder the matrix, the higher becomes the strain concentration factor. This result also indicates that, if the hard matrix is broken prior to the fibre, the strain concentration is high. In case (b), where the matrix is not cut, the matrix acts to reduce the strain concentration factor on the neighbouring fibres. On the other hand, in cases (a) and (c), where the matrix is cut, the cut matrix acts to raise the strain concentration factor on the neighbouring fibres. Thus the failure strain of the matrix is one of the strength-determining factors in addition to the failure strain of fibres.

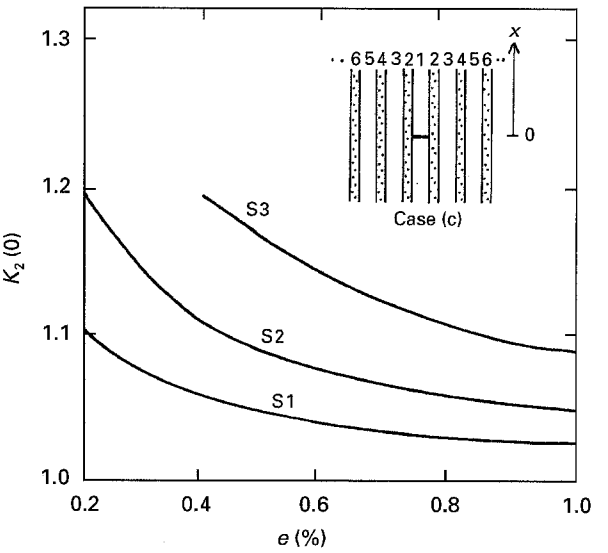

Figure 13 Influence of cut matrix on the strain concentration factor of neighbouring fibres, $K_2(0)$.

4. Conclusion

In order to calculate the stress disturbances arising from cut fibres and matrix in unidirectional metal matrix composites, a new calculation method, based on the shear lag analysis, has been presented. By using the present method, the strain concentration factor in elements ahead of cut elements, and the shear stress at the interface, were clarified in a quantitative manner.

Acknowledgement

The authors thank the Ministry of Education, Science and Culture of Japan for a grant-in-aid for Scientific Research (no. 06452320).

References

1. J. M. HEDGEPETH, NASA TN D-882 (1961).
2. G. W. ZENDER and J. W. DEATON, NASA TN D-1609 (1963).
3. E. D. REEDY Jr, *J. Compos. Mater.* **18** (1984) 595.
4. J. M. HEDGEPETH and P. Van DIKE, *ibid.* **1** (1967) 294.
5. C. ZWEBEN, *Eng. Fract. Mech.* **6** (1974) 1.
6. E. D. REEDY Jr, *J. Mech. Phys. Solids* **28** (1980) 265.
7. J. G. GOREE and R. S. GROSS, *Eng. Fract. Mech.* **13** (1980) 563.
8. L. R. DHARANI, W. F. JONES and J. G. GOREE, *ibid.* **17** (1983) 555.
9. S. OCHIAI, K. ABE and K. OSAMURA, *Z. Metallkde.* **76** (1985) 299.
10. J. A. NARIN, *J. Compos. Mater.* **22** (1988) 561.
11. S. OCHIAI, K. SCHULTE and P. W. M. PETERS, *Compos. Sci. Technol.* **41** (1991) 237.
12. S. OCHIAI and K. OSAMURA, *J. Mater. Sci.* **21** (1986) 2744.
13. N. F. DOW, GEC Missile and Space Division, Report no. R63SD61 (1993).

Received 12 May 1994
and accepted 13 February 1996